



INFLUENCES OF INDENTATION AND SCRATCHING DEPTH ON MECHANICAL CHARACTERISTICS OF $\text{Cu}_{50}\text{Zr}_{50}$ AMORPHOUS ALLOY

Phan Thi Ha Linh, Dung-Tuan Truong, Xuan-Thang Nguyen, Anh-Son Tran*

Hung Yen University of Technology and Education

* Corresponding author: anhsontan89@gmail.com

Received: 15/02/2021

Revised: 20/04/2021

Accepted for publication: 05/06/2021

Abstract:

In this work, the indentation and scratching process was performed using molecular dynamics simulation to explore the mechanical characteristics of the $\text{Cu}_{50}\text{Zr}_{50}$ amorphous alloy. The influences of various indentation and scratching depths on the mechanical characteristics of the $\text{Cu}_{50}\text{Zr}_{50}$ amorphous alloy were analyzed through the surface morphology, pile-up height, mean pressure, machining forces, and resistance coefficient. The results exhibited that all of the machining zone, pile-up height, mean pressure, machining forces, and resistance coefficient increase as increasing the machining depth.

Keywords: $\text{Cu}_{50}\text{Zr}_{50}$ MGs, indentation, scratching, mean pressure.

1. Introduction

Mechanical properties and deformation mechanisms are very typical and exceedingly important factors used to evaluate the characteristics of the materials. These factors directly influence the workability of the materials. Therefore, the investigation and evaluation on the mechanistic characteristics of materials are very necessary. Many experimental studies have been conducted to investigate the mechanical properties and the deformation mechanism of materials with different testing methods [1,2]. However, the sizes of the samples in the experimental studies are still quite large, in the microscale or macroscale. To assess the properties of materials more deeply and more accurately, the size of the material has been reduced to the nanoscale. The nanoscale is a major barrier for the performing of experimental studies, requiring an alternative method. With the strong development of computer technology, the molecular dynamics (MD) simulation method is an appropriate choice in simulating and evaluating the properties of nanomaterials. MD simulation method is simple and accurate in conducting the simulations with the testing processes are diverse such as shear, compression, indentation, tension, scratching, cutting.

In the modern industrial age today, metallic glasses (MGs) are widely used [3]. One of the most popular MG systems is the copper MGs type. Many systems of copper MGs have been created to study

the structural, dynamic properties such as Cu-Mg [4], Cu-Zr[5], Cu-Ta [6], Cu-Ni [7]. Among these copper MGs systems, Cu-Zr MGs have emerged as the promising immiscible alloy systems for applications in electrical engineering, magnetic-sensing, chemical, and structural materials. The indentation and scratching processes are usually performed to study the mechanical properties and deformation mechanisms of materials, however, the combination of these two processes is scarce, especially with Cu-Zr MGs.

In this work, the mechanical properties and deformation mechanisms of $\text{Cu}_{50}\text{Zr}_{50}$ MGs systems are analyzed and evaluated through the combination of indentation and scratching processes using MD simulation. The machining processes are simulated with different indenter radius. The results will supply a more penetrating understanding of the mechanistic abilities of $\text{Cu}_{50}\text{Zr}_{50}$ MGs.

2. Methodology

The structure of a $\text{Cu}_{50}\text{Zr}_{50}$ MGs model at room temperature is created from the simulation of the melting and quenching process. Firstly, the model is heated up to 2128 K (melting point of Zr component) at a heating rate of 2 K/ps. Then, the thermal equilibration process is kept at 2128 K for 500 ps. Finally, the model is cooled down to 300 K at a high cooling rate of 5 K/ps and then equilibrated at 300 K for 500 ps.

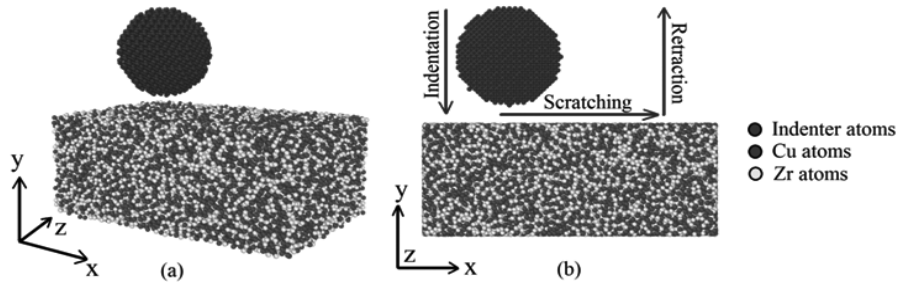


Figure 1. The $\text{Cu}_{50}\text{Zr}_{50}$ MGs model for the indentation, scratching, and retraction system

Figure 1 shows the $\text{Cu}_{50}\text{Zr}_{50}$ MGs model for the machining process. The machining system consists of a sphere diamond indenter and a $\text{Cu}_{50}\text{Zr}_{50}$ MGs specimen. The machining process is divided into three stages including indentation, scratching, and retraction. The indenter is considered an ideal rigid body to simplify the machining problem and focus on the deformation of the $\text{Cu}_{50}\text{Zr}_{50}$ MGs specimen. The indenter radius is 2.5 nm. The various machining depths are 1, 1.5, 2, 2.5, and 3 nm. The dimensions of the $\text{Cu}_{50}\text{Zr}_{50}$ MGs specimen are 15 nm (length) \times 6 nm (height) \times 10 nm (width) corresponding to x -, y -, and z -axis, respectively. The periodic boundary conditions are determined in the x -, and z -axis, while the free boundary is applied along the y -axis. The NVT (canonical ensemble) is used in the simulation. The initial distance between the indenter and the surface of the specimen is 1 nm. The machining process begins by the indentation stage with a machining depth of 2 nm and the indentation velocity of 50 m/s along the y -axis. Then, the scratching stage is performed with a scratch distance of 5 nm and a scratch velocity of 50 m/s along the x -axis. Finally, the indenter retracts to the original position at a retraction velocity of 100 m/s.

The EAM potential [8] is employed to depict the interaction between Cu and Zr atoms. The atoms interaction between the indenter and $\text{Cu}_{50}\text{Zr}_{50}$ MGs is employed by the Lennard-Jones (LJ) potential [4]. The indenter is set as a rigid body, therefore the interaction between C atoms of the indenter is ignored.

The mean pressure value (H) is determined as

$$H = \frac{F_{max}}{A_c} \quad (1)$$

where F_{max} is the maximum normal force, A_c is the contact area between the indenter and specimen in the indentation stage. A_c is calculated as

$$A_c = \pi R h_c \quad (2)$$

where h_c is the indentation depth. The resistance coefficient (μ) is determined as follows:

$$\mu = \frac{F_t}{F_n} \quad (3)$$

where F_t and F_n are the tangential and normal forces in the scratching stage, respectively.

The LAMMPS is applied to create all MD simulations. The OVITO is used to exhibit the processing data from MD simulations.

3. Results and discussion

3.1. Mechanical response of $\text{Cu}_{50}\text{Zr}_{50}$ amorphous alloy

The machining depth is the maximum depth attained in the indentation stage and scratching stage. To study the effects of machining depth on indentation and scratching characteristics of the $\text{Cu}_{50}\text{Zr}_{50}$ MGs, five machining depth values are selected as 1, 1.5, 2, 2.5, and 3 nm, respectively. The machining velocity is 50 m/s and the temperature is 300 K.

Figure 2(a) displays the lateral cross-sectional view of the pile-up and groove formed after the retraction of the indenter for the cases of different machining depths. Machining zone and pile-up height significantly increase with the increase of the machining depth. Corresponding, the chipping volume is also clearly larger and more chippings are generated around the groove as shown in Figure 2(b). That means the increase of the machining depth affects the indentation and scratching characteristics of the $\text{Cu}_{50}\text{Zr}_{50}$ MGs. With the relatively deeper machining depth, the contact area between the specimen and indenter becomes larger, leads to a groove zone is greater. Furthermore, more removed materials are extruded around the indenter and then emerge on the surface with deeper depth, resulting in the pile-up formation on the surface is stronger.

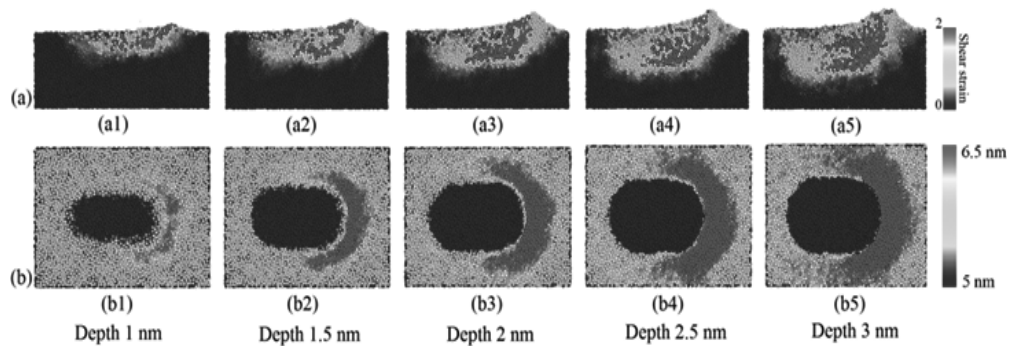


Figure 2. The lateral cross-sectional-view of the pile-up and groove formed after the retraction of the indenter (a) and the surface morphology (b) of the $\text{Cu}_{50}\text{Zr}_{50}$ MGs for the cases with different machining depths

A comparison between maximum pile-up height values of the $\text{Cu}_{50}\text{Zr}_{50}$ MGs during the indentation and scratching process at different machining depths is shown in Figure 3. The maximum pile-up height is 6, 9, 14, 16, and 18 Å corresponding to the machining depths of 1, 1.5, 2, 2.5, and 3 nm, respectively.

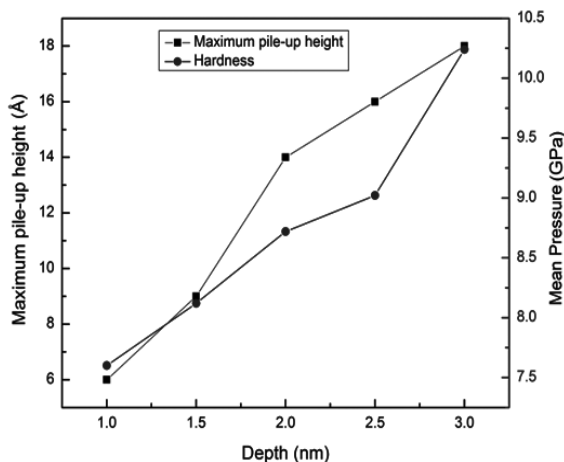


Figure 3. The maximum pile-up height and the mean pressure of the $\text{Cu}_{50}\text{Zr}_{50}$ MGs at different machining depths

A typical factor to assess the mechanical properties of the materials is mean pressure. The mean pressure values of the $\text{Cu}_{50}\text{Zr}_{50}$ MGs at different machining depths under the indentation process are presented in Figure 3. The mean pressure values are 7.60, 8.12, 8.72, 9.02, and 10.24 GPa corresponding to machining depths of 1, 1.5, 2, 2.5, and 3 nm, respectively. Heretofore, many nanoindentation tests have confirmed that the mean pressure significantly increases as the indentation size reduces. This phenomenon is

regularly called the indentation size effect (ISE). A profound explanation of the ISE encountered in mean pressure at the nanoscale from the spherical indenters has been launched by Hussain et al. [9]. Also, an ISE analytical model that can anticipate the equivalent mean pressure in the nanoindentation with the spherical indenter has been proposed. However, there are non-standard results were reported according to previous studies of the ISE that the mean pressure becomes higher with the deeper indentation depth for very small indentation depth. This phenomenon was called the inverse ISE phenomenon. The reason can be explained that the deformations form over a relatively small volume at a very small indentation depth, leading to the formation of a high density of the deformations. These deformations hinder deeper penetration of the indenter, thereby the apparent mean pressure of the material increases as indentation depth increases. The deformation density is the highest at a maximum indentation depth of 2 nm, resulting in the mean pressure is greater than that in the other cases in this study.

3.2. The effects of different machining depths on the force and resistance coefficient

Figure 4 shows the normal (F_n) and tangential (F_t) forces diagram of the $\text{Cu}_{50}\text{Zr}_{50}$ MGs during the indentation (stage 1), scratching (stage 2), and retraction (stage 3) process at different machining depths. In the first period of the indentation process and the final period of the retraction process, there is no impact between the indenter and the sample, thus the F_n and F_t values are zero. Under

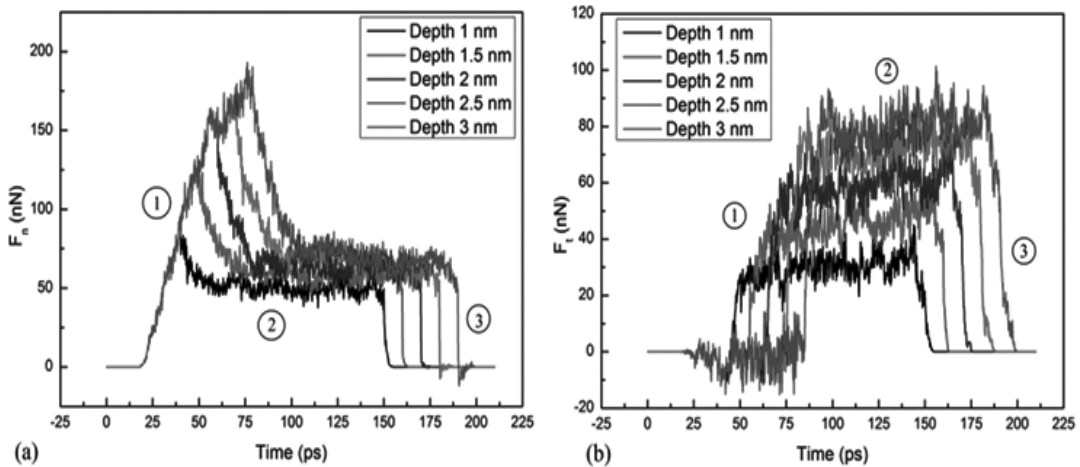


Figure 4. (a) Normal and (b) tangential force diagram of the $\text{Cu}_{50}\text{Zr}_{50}$ MGs during the indentation, scratching, and retraction process at different machining depths

the machining process when the depth increases, the amount of extruded material is intensified, leading to the necessary force required to process materials also increased. Therefore, the force value becomes greater as increasing machining depth. This phenomenon can be observed in both normal and tangential forces diagrams in Figure 4(a) and Figure 4(b), respectively.

During the indentation stage, the normal force F_n rapidly increases to the peak value, while the tangential force F_t fluctuates slightly around zero. However, after the beginning of the scratching stage, the tangential force F_t rises strongly due to the formation of the chips are started, while the normal force F_n suddenly decreases because of the contact area between the indenter and the sample reduces. The contact area reduction is due to the kinematics of the process. A gap is formed between the backside of the indenter and the substrate at the beginning of the scratching stage. Then, a stable phase for both F_n and F_t is observed and maintained until the scratching process ends. However, the strong fluctuations of F_n and F_t happen in this stable phase in all cases. This is due to the oscillation is generated by the continuous impact between the indenter and the substrate, leading to the F_n and F_t also change. The change in the tangential force is more intense than that in the normal force. Finally, both F_n and F_t rapidly drop to zero when the indenter retracts from the substrate. There is no difference between F_n and F_t in all simulations.

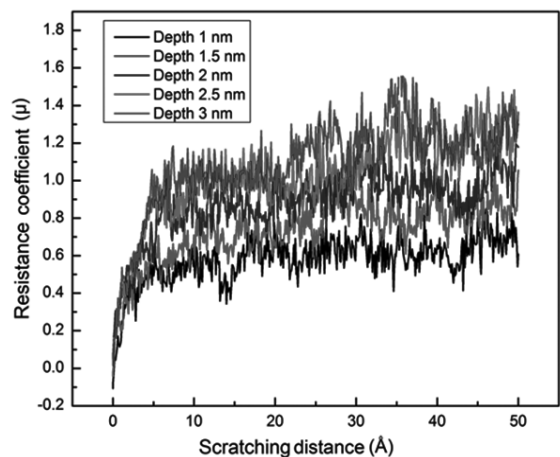


Figure 5. Resistance coefficient of the $\text{Cu}_{50}\text{Zr}_{50}$ MGs at different machining depths under the scratching process

The resistance coefficient is determined as the ratio between F_t and F_n , which is calculated to depict the mechanical response of $\text{Cu}_{50}\text{Zr}_{50}$ MGs under scratching. The resistance coefficient diagram of $\text{Cu}_{50}\text{Zr}_{50}$ MGs at different machining depths under the scratching process is shown in Figure 5. In all five different machining depth cases, the curves present common features: first, the resistance coefficient increases suddenly in the beginning phase of the scratching process, and then vibrates strongly around a constant average value when scratching is stable. It can be observed that the resistance coefficient is higher with the deeper machining depth. The resistance coefficient values

are smaller than 1 for the machining depths of 1, 1.5, and 2 nm, while these values are greater than 1 for the machining depths of 2.5 and 3 nm. The resistance coefficient tends to increase as increasing scratching distance. The difference in the resistance coefficient above is due to the effect of machining depth. With a deeper depth, greater energy is required to remove materials in the scratching process. This also indicates that the depth affects the deformation mechanism and mechanical properties of the $\text{Cu}_{50}\text{Zr}_{50}$ MGs during the machining process.

4. Conclusion

In the cases of different machining depths with $\text{Cu}_{50}\text{Ta}_{50}$ MGs specimens, the machining zone, pile-up height, mean pressure, force, and resistance coefficient significantly increase as the increasing machining depth.

Acknowledgments

The authors acknowledge the support by Hung Yen University of Technology and Education, Vietnam under grant numbers UTEHY.L.2021.12.

References

- [1]. Ryou, K. H., Nambu, S., & Koseki, T., Effect of carbon content on selection of slip system during uniaxial tensile deformation of lath martensite. *Materials Science and Engineering: A*, **777**, 139090, 2020.
- [2]. Sun, G., Chen, D., Huo, X., Zheng, G., & Li, Q., Experimental and numerical studies on indentation and perforation characteristics of honeycomb sandwich panels. *Composite Structures*, **184**, 110-124, 2018.
- [3]. Hilzinger, H., Applications of metallic glasses in the electronics industry. *IEEE Transactions on Magnetics*, **21(5)**, 2020-2025, 1985.
- [4]. Bailey, N. P., Schiøtz, J., & Jacobsen, K. W. Simulation of Cu-Mg metallic glass: Thermodynamics and structure. *Physical Review B*, **69(14)**, 144205, 2004.
- [5]. Wang, Y., Zhang, J., Wu, K., Liu, G., Kiener, D., & Sun, J., Nanoindentation creep behavior of Cu–Zr metallic glass films. *Materials Research Letters*, **6(1)**, 22-28, 2018.
- [6]. Bhatia, M. A., Rajagopalan, M., Darling, K. A., Tschopp, M. A., & Solanki, K. N. (2017). The role of Ta on twinnability in nanocrystalline Cu–Ta alloys. *Materials Research Letters*, **5(1)**, 48-54.
- [7]. Kazanc, S. (2007). Molecular dynamics study of pressure effect on crystallization behaviour of amorphous CuNi alloy during isothermal annealing. *Physics Letters A*, **365(5-6)**, 473-477.
- [8]. Ye, Y., Yang, X., Wang, J., Zhang, X., Zhang, Z., & Sakai, T. (2014). Enhanced strength and electrical conductivity of Cu–Zr–B alloy by double deformation–aging process. *Journal of Alloys and Compounds*, **615**, 249-254.
- [9]. Hussain, F., Imran, M., Rashid, M., Ullah, H., Shakoor, A., Ahmad, E., & Ahmad, S. A. (2014). Molecular dynamics simulation of mechanical characteristics of CuZr bulk metallic glasses using uni-axial tensile loading technique. *Physica Scripta*, **89(11)**, 115701.

ẢNH HƯỞNG CỦA CHIỀU SÂU TẠO LỖM VÀ CÀO XƯỚC ĐẾN TÍNH CHẤT CƠ HỌC CỦA HỢP KIM VÔ ĐỊNH HÌNH $\text{Cu}_{50}\text{Zr}_{50}$

Tóm tắt:

Trong bài báo này, quá trình tạo vết lõm và cào xước được thực hiện sử dụng phương pháp mô phỏng động lực học phân tử để nghiên cứu các đặc tính cơ học của hợp kim vô định hình $\text{Cu}_{50}\text{Zr}_{50}$. Ảnh hưởng của chiều sâu tạo lõm và cào xước đến các đặc tính cơ học của hợp kim vô định hình $\text{Cu}_{50}\text{Zr}_{50}$ được phân tích thông qua hình thái bề mặt, chiều cao chất đống, áp lực ấn trung bình, lực gia công, và hệ số cản được đánh giá. Kết quả cho thấy rằng vùng gia công, chiều cao chất đống, áp lực ấn trung bình, lực gia công và hệ số cản đều tăng khi tăng chiều sâu gia công.

Từ khóa: Hợp kim vô định hình $\text{Cu}_{50}\text{Zr}_{50}$, quá trình tạo lõm, quá trình cào xước, hệ số cản.